Transition Met Chem
DOI 10.1007/s11243-016-0047-2

Copper complexes of pyridyl–tetrazole ligands with pendant amide and hydrazide arms: synthesis, characterization, DNA-binding and antioxidant properties

Santhosh Reddy Kasi Reddy[1] · Surendrababu Manabolu Surya[1] · Mustafa Shaik[1] · Phani Raja Kanuparthy[1]

Received: 31 December 2015 / Accepted: 24 March 2016

Abstract Pyridyl–tetrazole ligands 2-(5-(pyridin-2-yl)-1H-tetrazol-1-yl)acetamide (**L1**), 2-(5-(pyridin-2-yl)-2H-tetrazol-2-yl)acetamide (**L2**), 2-(5-(pyridin-2-yl)-1H-tetrazol-1-yl)acetohydrazide (**L3**) and 2-(5-(pyridin-2-yl)-2H-tetrazol-2-yl)acetohydrazide (**L4**) have been prepared and coordinated with $CuCl_2{\cdot}2H_2O$ to furnish the corresponding complexes [**Cu(L1)$_2$**]–[**Cu(L4)$_2$**]. EPR spectra of the complexes are characteristic of square planar geometries, with nuclear hyperfine spin 3/2. DNA-binding studies using UV–Vis absorption spectroscopy, viscosity and thermal denature studies revealed that all of these complexes are avid binders of calf thymus DNA. The antioxidant properties of the free ligands and the Cu(II) complexes were investigated using the *p*-nitrosodimethyl aniline hydroxyl radical scavenging method, and [**Cu(L4)$_2$**] was found to show the highest activity.

Introduction

Tetrazoles exhibit various biological activities and act as a pharmacophore for the carboxylate group [1]. Recently, there has been a growing demand for pyridyl tetrazoles as components of metal–organic frameworks (MOFs), which have attracted much attention in the past decade as a result of their interesting structural topographies as well as their useful properties and applications, including storage of gases, catalysis, drug delivery, magnetism and luminescence [2]. The metal complexes of tetrazoles find a wide range of biochemical and pharmaceutical applications by virtue of their high physiological activity and low toxicity [3]. Tetrazoles are important tools in synthetic organic chemistry and also used as precursors of carbenes in flash pyrolysis [4]. The pharmacological applications of tetrazoles with glycosidase inhibitory, antihypertensive, anti-inflammatory, antibacterial, antifungal, analgesic, antinociceptive, anticancer, anticonvulsant, antidiabetic, antiulcer and antitubercular activities have been reported [5]. Tetrazoles play a significant role in coordination chemistry as ligands, as metabolically stable surrogates for carboxylic acid groups in medical chemistry and as high-energy materials [6]. Tetrazole resembles the carboxylic group in its acidic characteristics and is metabolically stable [7]. Applications of 5-substituted-1*H*-tetrazoles as lipophilic spacers have been reported [8]. In addition, pyridines are associated with diverse biological activities [9]. In continuation of our ongoing research [10], we have prepared pyridyl tetrazoles with pendant acetamide and acetohydrazide groups (Scheme 1) and investigated their copper(II) complexes (Scheme 2). The results of our investigations are reported in this paper.

Experimental

Materials and measurements

Picolinonitrile **1** was purchased from Sigma-Aldrich. The solvents used in the synthesis of the ligands and their complexes were distilled before use. All other chemicals were of AR grade and were used without further purification. Hydrazine hydrate is a hazardous compound, and its MSDS data sheet was referred to prior to its use. All melting points were obtained on an Elico instrument, India

✉ Mustafa Shaik
mustaff_02@yahoo.co.in

[1] Department of Chemistry, GITAM University Hyderabad Campus, Hyderabad 502329, India

Published online: 16 April 2016

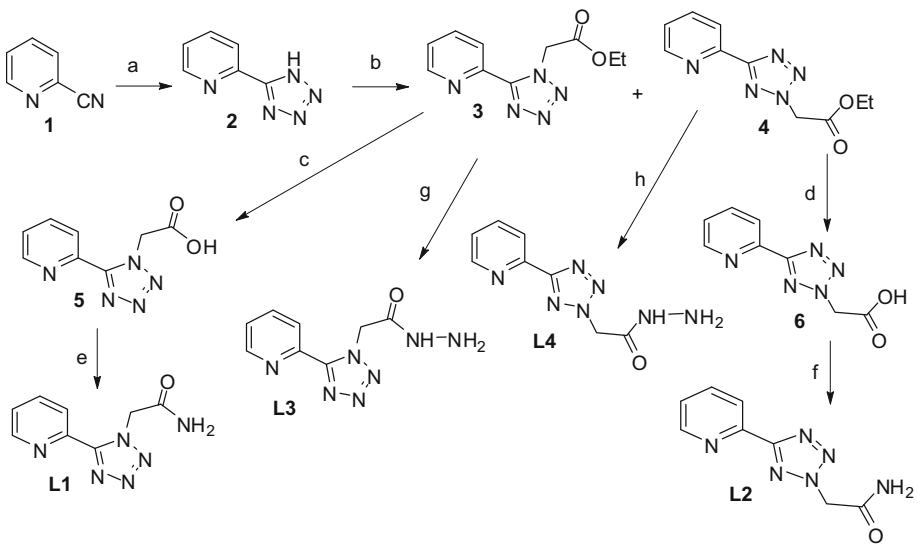

Scheme 1 Synthesis of **L1–L4**. Reagents and conditions: *a* NaN_3, LiCl, NH_4Cl, DMF, reflux, 10 h; *b* ethylbromo acetate, DMF, 70 °C, 8 h; *c*, *d* aq. NaOH (1 N), MeOH, r.t., 6 h; *e*, *f* BOC anhydride, pyridine, $(NH_4)_2CO_3$, dioxane, r.t., 8 h; *g*, *h* hydrazine hydrate, EtOH, 80 °C, 10 h

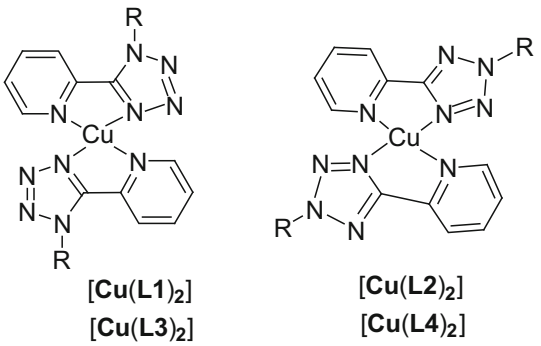

Scheme 2 Structural formulae of the complexes. **L1**, **L2**, R = $–CH_2N(O)NH_2$; **L3**, **L4**, R = $–CH_2N(O)NHNH_2$

(Model MP96), and are uncorrected. Mass spectra were obtained on a PeSciex API 2000 eV spectrometer and Q1MSQ1/auto-injection mass spectra. ^1H and ^{13}C NMR spectra were recorded on a Bruker Top Spin Instrument. IR spectra were recorded using an Alpha T OPUS spectrometer. Elemental analysis (C, H and N) was obtained using a PerkinElmer 2400 elemental analyzer. Magnetic moments were determined in the polycrystalline state on a PAR model-155 vibrating sample magnetometer operating at field strength of 2–8 kg. High-purity Ni metal (saturation moment 55 emu g^{-1}) was used as standard. EPR spectra were recorded on a Varian E-122 X-band spectrometer at liquid nitrogen temperature in DMF.

General procedure for the synthesis of 3 and 4

To a solution of tetrazole **2** (1 g, 6.8 mmol) in DMF (15 ml) was added ethylbromo acetate (0.75 ml, 6.8 mmol). The mixture was stirred for 8 h at 70 °C and then diluted with ethyl acetate (50 ml). The organic layer was washed successively with saturated $NaHCO_3$ (50 ml) and then water (40 ml × 3) followed by brine solution (40 ml). The organic layer was dried over $MgSO_4$ and filtered, and the solvent was evaporated under reduced pressure to afford a gummy brown liquid, which was purified by column chromatography using 17 % EtOAc in hexane (V/V) to afford the esters **3** and **4**.

Ethyl 2-(5-(pyridin-2-yl)-1H-tetrazol-1-yl)acetate (**3**) [2] Yellowish solid; Yield: 0.45 g (28 %). Yellow solid. M.p. 54–57 °C. Anal. Calc. for $C_{10}H_{11}N_5O_2$ (233.23): % of C, 51.5; H, 4.7; N, 30.0. Found: % of C, 51.5; H, 4.7; N, 30.0. ^1H NMR ($CDCl_3$, 300 MHz): δ 8.66 (d, 1H, $J = 3.3$ Hz), 8.43 (d, 1H, $J = 8.1$ Hz), 7.92 (dt, 1H, $J = 7.8$, 1.8 Hz), 7.48–7.41 (m, 1H), 5.75 (s, 2H), 4.19 (q, 2H, 6.9 Hz), 1.21 (t, 3H, $J = 6.9$ Hz) ppm.

Ethyl 2-(5-(pyridin-2-yl)-2H-tetrazol-2-yl)acetate (**4**) [2] Yellowish solid Yield: 0.80 g (50 %). White solid. M.p. 94–98 °C. Anal. Calc. for $C_{10}H_{11}N_5O_2$ (233.23): % of C, 51.5; H, 4.7; N, 30.0. Found: % of C, 51.5; H, 4.7; N, 30.0. ^1H NMR ($CDCl_3$, 300 MHz): δ 8.79 (d, 1H, $J = 4.8$ Hz), 8.28 (d, 1H, $J = 7.8$ Hz), 7.88 (td, 1H, $J = 7.8$, 1.8 Hz), 7.42 (m, 1H), 5.50 (s, 2H), 4.29 (q, 2H, $J = 7.2$ Hz), 1.29 (t, 3H, $J = 7.2$ Hz) ppm.

General procedure for the synthesis of 5 and 6

To a methanolic (21 ml) solution of ester **3** or **4** (0.5 g, 2.14 mmol), 2 ml of aq. NaOH (1 N) was added and the resulting solution was stirred for 6 h at room temperature, resulting in the formation of a white precipitate. The reaction was quenched with 3–4 drops of acetic acid, and 10 ml of ethyl acetate was added. The mixture was filtered and the residue washed with ethyl acetate (20 ml); the colorless residue was collected and dried in air.

2-(5-(Pyridin-2-yl)-1H-tetrazole-1-yl)acetic acid (**5**): Colorless solid; Yield: 400 mg (91 %). M.p. 284–287 °C. Anal. Calc. for $C_8H_7N_5O_2$ (205.17): % of C, 46.8; H, 3.4; N, 34.1. Found: % of C, 46.8; H, 3.4; N, 34.1. ^{1}H NMR ($CDCl_3$, 300 MHz): δ 8.72 (t, 1H, $J = 4.8$,3.9 Hz), 8.12 (d, 1H, $J = 7.8$ Hz), 8.03 (m, 1H), 7.58 (m, 1H), 5.45 (s, 2H) ppm. ^{13}C NMR ($CDCl_3$, 65 MHz): δ 172.5, 153.1, 149.9, 143.2, 138.4, 126.3, 124.4, 52.9. ESI–MS: *m/z* 204 (M − 1).

2-(5-(Pyridin-2-yl)-2H-tetrazole-2-yl)acetic acid (**6**): Colorless solid; Yield: 0.38 g (86 %). M.p. 277–279 °C. Anal. Calc. for $C_8H_7N_5O_2$ (205.17): % of C, 46.8; H, 3.4; N, 34.1. Found: % of C, 46.8; H, 3.4; N, 34.1. ^{1}H NMR ($CDCl_3$, 300 MHz): δ 8.73 (d, 1H, $J = 4.5$ Hz), 8.11 (d, 1H, $J = 8.1$ Hz), 7.98 (td, 1H, $J = 7.5$, 1.5 Hz), 7.52 (m, 1H), 4.97 (s, 2H) ppm. ^{13}C-NMR ($CDCl_3$, 75 MHz): δ 172.19, 164.49, 150.15, 145.47, 139.25, 126.59, 123.58, 56.71 ppm. ESI–MS: *m/z* 204 (M − 1).

General procedure for the synthesis of L1 and L2

To a solution of acid **5 or 6** (0.5 g, 2.44 mmol) in dioxane (30 ml), a mixture of BOC anhydride (0.85 ml, 3.7 mmol) and pyridine (0.24 ml, 2.93 mmol) was added at room temperature. The mixture was stirred for 0.5 h, and then, ammonium carbonate (281 mg, 2.93 mmol) was added, and the resulting solution was stirred for 8 h. The reaction mixture was filtered, and the filtrate was extracted with ethyl acetate (30 ml). The organic layer was washed with water (30 ml × 3) followed by brine. The organic layer was dried over Na_2SO_4 and filtered, and the solvent was removed under reduced pressure to afford a crude product, which was triturated with diethyl ether to furnish a colorless solid.

Ethyl 2-(5-(pyridin-2-yl)-1H-tetrazol-1-yl)acetamide (**L1**): Colorless solid; Yield: 0.25 g (50 %). M.p. 97–99 °C. Anal. Calc. for $C_8H_8N_6O$ (204.19): % of C, 47.0; H, 3.9; N, 41.2. Found: % of C, 47.0; H, 3.9; N, 41.1. ^{1}H NMR ($CDCl_3$, 300 MHz): δ 8.73 (t, 1H, $J = 4.2$, 3.3 Hz), 8.16 (d, 1H, $J = 7.8$ Hz), 8.05 (m, 1H), 8.01 (br. s, 1H), 7.59 (m, 2H), 6.14 (br. s, 1H), 6.13 (s, 2H) ppm. ^{13}C-NMR ($CDCl_3$, 75 MHz): δ 172.6, 153.3, 149.4, 143.6, 138.4, 126.3, 124.6, 53.1 ppm. MS: *m/z* 205 (M + 1).

Ethyl 2-(5-(pyridin-2-yl)-2H-tetrazol-2-yl)acetamide (**L2**): Colorless solid; Yield: 0.36 g, (72 %). M.p. 98–103 °C. Anal. Calc. for $C_8H_8N_6O$ (204.19): % of C, 47.0; H, 3.9; N, 41.2. Found: % of C, 47.0; H, 3.9; N, 41.1. ^{1}H NMR ($CDCl_3$, 300 MHz): δ 8.75 (t, 1H, $J = 4.2$, 3.3 Hz), 8.15 (d, 1H, $J = 7.8$ Hz), 8.02 (td, 1H, $J = 7.5$, 1.5 Hz), 7.90 (br-s, 1H), 7.56 (m, 2H), 6.16 (br-s, 1H), 5.51 (s, 2H) ppm. ^{13}C-NMR ($CDCl_3$, 75 MHz): δ 172.2, 164.5, 150.2, 145.5, 139.3, 126.6, 123.6, 56.7 ppm; MS: *m/z* 205 (M + 1).

General procedure for the synthesis of L3 and L4

To an ethanolic solution (10 ml) of ester **3** or **4** (0.5 g, 2.14 mmol), hydrazine hydrate (0.2 ml, 4.28 mmol) was added, and the resulting solution was stirred for 10 h at 80 °C. The solvent was removed under reduced pressure, and the crude material was triturated with diethyl ether to afford a colorless solid.

2-(5-(Pyridin-2-yl)-1H-tetrazol-1-yl)acetohydrazide (**L3**): Colorless solid; Yield: 0.32 g (68 %). M.p. 185–187 °C. Anal. Calc. for $C_8H_9N_7O$ (219.20): % of C, 43.8; H, 4.1; N, 44.7. Found: % of C, 43.8; H, 4.1; N, 44.7. ^{1}H NMR (DMSO-D6, 300 MHz): δ 9.48 (br-s, 1H–NH), 8.72 (d, 1H, $J = 4.5$ Hz), 8.30 (d, 1H, $J = 12.9$ Hz), 8.08 (dt, 1H, $J = 7.8$, 1.8 Hz), 7.62 (dd, 1H, $J = 4.8$, 1.8 Hz), 5.64 (s, 2H), 4.29 (br-s, 2H–NH2) ppm. ^{13}C-NMR (DMSO-D6, 75 MHz): δ 166.7, 152.6, 149.7, 144.2, 138.2, 125.9, 123.7, 48.6 ppm; MS: *m/z* 220 (M + 1).

2-(5-(Pyridin-2-yl)-2H-tetrazol-2-yl)acetohydrazide (**L4**): Colorless solid; Yield: 0.32 g (68 %). M.p. 168–171 °C. Anal. Calc. for $C_8H_9N_7O$ (219.20): % of C, 43.8; H, 4.1; N, 44.7. Found: % of C, 43.8; H, 4.1; N, 44.7. ^{1}H NMR (DMSO-D6, 300 MHz): δ 10.8 (br-s, 1H–NH), 8.76 (d, 1H, $J = 4.5$ Hz), 8.13 (d, 1H, $J = 7.8$ Hz), 8.02 (dt, 1H, $J = 7.5$, 1.5 Hz), 7.57 (dd, 1H, $J = 4.8$, 1.0 Hz), 5.88 (s, 2H), 3.56 (br-s, 2H–NH_2) ppm. ^{13}C-NMR (DMSO-D6, 75 MHz): δ 166.5, 164.2, 150.4, 145.6, 139.3, 126.2, 123.3, 51.4 ppm; MS: *m/z* 220 (M + 1).

General procedure for synthesis of the complexes

To a solution of **L1** to **L4** (0.487 mmol) in methanol (10 ml), $CuCl_2{\cdot}2H_2O$ (0.244 mmol) was added, and the resulting solution was stirred for 2 h at 70 °C. The resulting mixture was allowed to cool, and the solvent was evaporated slowly in the hope of obtaining crystals. But after 7 days, the evaporation afforded only amorphous green solids. These solids were triturated with diethyl ether and used without further purification.

[**Cu(L1)$_2$**]: 189 mg, 0.4 mmol; IR (KBr, cm^{-1}): 3445 (w), 2938 (s), 2027 (s), 1636 (m), 1575 (m), 1400 (s), 1316 (s), 1294 (s), 1084 (s), 985 (s), 896 (s). Anal. calc. for $C_{16}H_{16}N_{12}O_2Cu$ (472): % of C, 40.7; H, 3.4; N, 35.6; Found: % of C, 40.3; H, 3.3; N, 35.5. ESI–MS: *m/z* 472 (M + 1).

[**Cu(L2)$_2$**]: 195 mg, 0.42 mmol; IR (KBr, cm^{-1}): 3448 (w), 2981 (s), 2067 (s), 1635 (m), 1568 (m), 1397 (s), 1252 (s), 1168 (s), 1053 (s), 789(s), $C_{16}H_{16}N_{12}O_2Cu$ (472): % of C, 40.7; H, 3.4; N, 35.6. Found: % of C, 40.3; H, 3.4; N, 35.5. ESI–MS: *m/z* 472 (M + 1).

[**Cu(L3)$_2$**]: 210 mg, 0.42 mmol; IR (KBr, cm^{-1}): 3413 (w), 3254 (w), 2033 (s), 1763 (m), 1637 (m), 1618 (m), 1455 (s), 1309 (s), 1294 (s), 1229 (s), 1110 (s), 1013 (s), 788 (s), 748 (m). Anal. calc. for $C_{16}H_{18}N_{14}CuO_2$ (502): % of C, 38.3; H, 3.6; N, 39.0. Found: % of C, 38.1; H, 3.5; N, 39.0. ESI–MS: *m/z* 502 (M + 1).

[Cu(L4)$_2$]: 195 mg, 0.39 mmol; IR (KBr, cm^{-1}): 3453 (w), 3254 (w), 2042 (s), 1753 (m), 1628 (m), 1592 (m), 1438 (s), 1395 (s), 1313 (s), 1170 (s), 1113 (s), 1013 (s), 786 (s), 728 (m). Anal. calc. for $C_{16}H_{18}N_{14}CuO_2$ (502): % of C, 38.3; H, 3.6; N, 39.0. Found: % of C, 38.2; H, 3.5; N, 39.0. ESI–MS: *m/z* 502 (M + 1).

Measurement of antioxidant activity

To a solution containing $FeCl_3$ (0.1 mM, 0.5 ml), EDTA (0.1 mM, 0.5 ml), ascorbic acid (0.1 mM, 0.5 ml), hydrogen peroxide (2 mM, 0.5 ml) and *p*-nitrosodimethyl aniline (0.01 mM, 0.5 ml) in phosphate buffer (p^H 7.4, 20 mM) were added various concentrations of the test compounds in distilled DMSO to produce a final volume of 3 ml. The absorbance of the solution was then measured at 440 nm, and the radical scavenging activity was calculated using the following equation;

$$\text{p} - \text{NDA radical scavenging activity}\,(\%) = \frac{[A(\text{sample}) - A(\text{standard})]}{[A(\text{sample})]} \times 100 \quad (1)$$

where A = Absorbance.

DNA-binding experiments

All measurements with CT-DNA were taken in Tris–HCl buffer 5 mM (pH 7.2), 50 mM NaCl. The UV absorbance ratio of the DNA at 260/280 was 1.8–1.9, indicating that the DNA was sufficiently free of protein [11]. The concentration of CT-DNA per nucleotide was determined from the absorption intensity at 260 nm with the known extinction coefficient of 6600 M^{-1} cm^{-1}. The absorption titrations were performed by adding increasing amounts of CT-DNA to a solution of the complex at a fixed concentration contained in a quartz cell and recording the UV–Vis spectrum after each addition. The absorption of CT-DNA was subtracted by adding the same amount to the blank. The data were then fitted to Eq. (2) to obtain the intrinsic binding constant, K_b [12].

$$[\text{DNA}]/(\varepsilon_a - \varepsilon_f) = [\text{DNA}]/(\varepsilon_b - \varepsilon_f) + 1/K_b(\varepsilon_b - \varepsilon_f) \quad (2)$$

where [DNA] is the molar concentration of CT-DNA, ε_a, ε_b and ε_f are apparent, free and bound metal complex extinction coefficients, respectively. Thus, K_b is the ratio of the slope to the y-intercept.

Results and discussion

Starting from the picolinonitrile **1**, the literature procedure was followed to give the tetrazole **2**, whose analytical data were comparable to the literature values [13, 14]. Tetrazole **2** on alkylation with ethylbromo acetate in dry DMF at 70 °C afforded regio-isomers **3** and **4** by alkylation at the tetrazole N(1) or N(2) positions, respectively (Scheme 1). The structures of the isomers were readily assigned by their ^{1}H NMR spectra. Compound **3** showed characteristic peaks at δ 5.75 (–N–CH_2–CO–), 4.19 (O–CH_2) and 1.21(–CH_3), which confirmed the formation of an ethyl ester. Similarly, compound **4** showed characteristic peaks at δ 5.5 (–N–CH_2–CO–), 4.29 (O–CH_2) and 1.29 (–CH_3). The ethyl esters were further confirmed by comparing the data with reported compounds [2]. The ethyl ester derivatives **3** and **4** were hydrolyzed to acid derivatives **5** and **6**, respectively, by treating with aqueous 1 N NaOH. The ^{1}H NMR spectra of **5** and **6** confirmed the absence of –OCH_2CH_3 peaks and upfield shifts of the N–CH_2 peaks. The acid derivatives were further characterized by their mass spectra, which showed M − 1 (negative mode) peaks at 204. The acid derivatives **5** and **6** on treatment with ammonium carbonate, BOC anhydride and pyridine in dry 1,4-dioxane afforded the respective acetamide ligands **L1** and **L2**. The formation of **L1** was confirmed by the observation of –CO–NH_2 signals at δ 8.01 and 6.14 ppm as broad singlets; similarly, **L2** showed broad singlets at δ 7.9 and 6.16 ppm. The mass spectra of both **L1** and **L2** showed M + H peaks at 205.

The acetohydrazide ligands **L3** and **L4** were prepared by reacting the ethylester derivatives **3** and **4** with hydrazine (Scheme 1). The hydrazide **L3** was characterized by ^{1}H NMR, which showed a characteristic –CO–NH peak as a broad singlet at δ 9.48 ppm. The hydrazide –NH_2 peak appeared as broad singlet at δ 4.29 ppm. The ^{1}H NMR spectrum of the hydrazide **L4** showed a characteristic –CO–NH peak at δ 10.8 ppm as a broad singlet, while the hydrazide –NH_2 peak gave a broad singlet at δ 3.56 ppm. The mass spectra of both **L3** and **L4** showed M + H peaks at 220.

The ^{1}H NMR spectra of all the compounds **3–6** and **L1–L4** all showed four signals corresponding to pyridyl protons. The ^{13}C NMR chemical shift values for the tetrazole quaternary carbon of each of these compounds were observed at ~153 ppm for the N(1)-isomers and at δ ~ 164 ppm for the N(2)-isomers.

The ligands **L1–L4** were treated with $CuCl_2{\cdot}2H_2O$, in refluxing methanol using a 1:2 meta/ligand ratio to give the corresponding complexes **[Cu(L)$_2$]** (Scheme 2). The physical properties of the complexes are given in Table 1. The elemental analyses of all four complexes showed 1:2 (metal/ligand) compositions. All of these complexes have magnetic moment values in the range of 1.84–1.92 BM, which is slightly higher than the spin-only values (1.73 μ_{eff}) expected for a d^9 copper(II) system [15].

The ESI mass spectra of the complexes were used to confirm their stoichiometries. The molecular ion peaks

Table 1 Physical properties of the complexes

Complex	Color	Melting point (°C)	μ_{eff} (BM)
[Cu(L1)$_2$]	Green	162–164	1.84
[Cu(L2)$_2$]	Green	158–160	1.92
[Cu(L3)$_2$]	Green	201–203	1.86
[Cu(L4)$_2$]	Green	194–198	1.90

Table 2 Electronic spectral data for the complexes

Complexes	MLCT (nm)	d–d (nm)
Cu(L1)$_2$	438 (8250)	655 (145)
Cu(L2)$_2$	430 (7400)	652 (130)
Cu(L3)$_2$	437 (8150)	650 (140)
Cu(L4)$_2$	445 (7840)	654 (150)

Extinction coefficients are given in the brackets

(M^+) of **[Cu(L1)$_2$]** and **[Cu(L2)$_2$]** were observed at $m/z = 472$ and those for **[Cu(L3)$_2$]** and **[Cu(L4)$_2$]** at 502, consistent with the proposed formulations.

The electronic spectra of these complexes recorded in DMF are summarized in Table 2. The spectra showed bands in the region of 430–450 nm with high molar extinction coefficients in the range of 8300–7300 M^{-1} cm^{-1}, which are assigned to metal-to-ligand charge transfer (MLCT) transitions ($n - \pi^*$). The single broadband observed in the region 655–650 nm is assigned to d–d transitions; these bands have low intensities, with molar extinction coefficients between 130 and 95 M^{-1} cm^{-1}. They are assigned to $^2E_g \rightarrow {}^2T_{2g}$ electronic transitions, suggesting a symmetrical square planar geometry for the copper(II) complexes [16, 17].

The IR spectral data for the complexes are summarized in Table 3. The free ligands **L1** and **L2** both show a broadband in range 3550–3100 cm^{-1} corresponding to $-NH_2$ of the amide/hydrazine group, plus amide peaks at 1681 and 1685 cm^{-1}, respectively. The equivalent at 1622 and 1642 cm^{-1} for the hydrazine ligands **L3** and **L4** is observed at lower frequencies. All of these peaks are shifted to lower frequencies in the copper complexes. The peaks at 1626–1534 cm^{-1} assigned to the pyridyl tetrazole group are also shifted to lower frequency in the complexes, indicating coordination of the pyridyl tetrazole rings with copper [18]. Additional peaks around 1395–1250 and 800–600 cm^{-1} are consistent with coordination of the pyridine ring to the metal. The relatively few bands observed in the spectra of the complexes suggest that they are symmetric in nature [19].

Table 4 EPR spectral assignments for the complexes at room temperature

Complexes	$g_{\|}$	$g_{\perp}$	g_{av}	G
[Cu(L1)$_2$]	2.16	2.05	2.10	3.306
[Cu(L3)$_2$]	2.14	2.04	2.09	3.652

The solid-state EPR spectra of **[Cu(L1)$_2$]** and **[Cu(L3)$_2$]** were recorded in the X-band region at 25 °C, and the data are summarized in Table 4. **[Cu(L1)$_2$]** and **[Cu(L3)$_2$]** exhibit $g_{\|}$ values of 2.16 and 2.18 and $g_{\perp}$ values of 2.05 and 2.06, respectively. In both cases, it is clear that $g_{\|} > g_{\perp} > 2.00$, suggesting that the unpaired electron lies predominantly in the $d^{22}_{x\text{-}y}$ orbital, which is the characteristic of square planar geometry in copper(II) complexes.

The geometric parameter G, which is a measure of the exchange interaction between the copper centers in the polycrystalline compound, was calculated using Eq. 3.

$$G = (g|| - 2.0023)/\left(g^{\perp} - 2.0023\right) \quad (3)$$

According to Hathaway and Tomlinson [20], if $G > 4.0$, the exchange interaction is negligible because the local tetragonal axes are aligned parallel or only slightly misaligned. If $G < 4.0$, exchange is considerable, and the local tetragonal axes are misaligned. The G values of **[Cu(L1)$_2$]** and **[Cu(L3)$_2$]** were obtained as 3.306 and 3.652, respectively, suggesting that there is no exchange interaction in these copper(II) complexes.

DNA-binding studies

The binding interactions of the complexes with CT-DNA were investigated by UV–Vis spectroscopy. The complexes were stable in Tris buffer solution [21] (refer Fig. 2S, supplementary information). The absorption spectra of the copper complexes were compared with and without CT-DNA at 400 nm (Fig. 1). The obtained UV–Vis data and the binding constants of these complexes are given in Table 5. Upon addition of increasing amounts of

Table 3 Selective I.R. bands cm^{-1}, of Cu(II) complexes with tentative assignments

Vibration	**L1**	**[Cu(L1)$_2$]**	**L2**	**[Cu(L2)$_2$]**	**L3**	**[Cu(L3)$_2$]**	**L4**	**[Cu(L4)$_2$]**
Amide/	1681	1636	1685	1635	–	–	–	–
Hydrazine	–	–	–	–	1622	1618	1642	1628
C=N (tetrazole)	1617	1575	1606	1568	1534	1455	1626	1592
C=C (tetrazole)	1498	1400	1486	1397	1471	1309	1508	1438
Py/M-Py	1392	1316	1334	1252	1433	1294	1443	1395

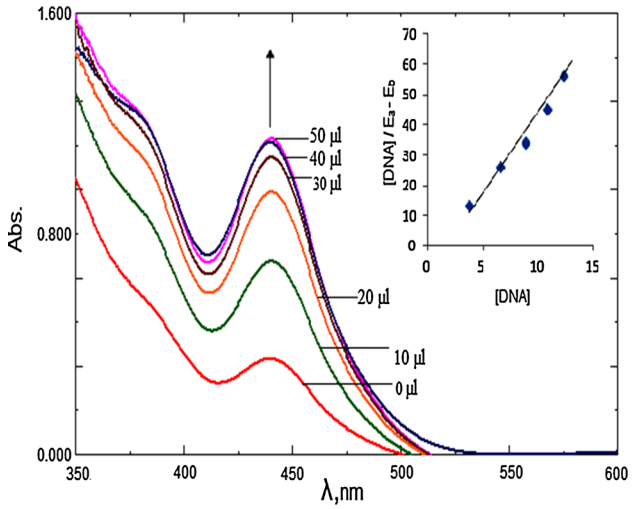

Fig. 1 UV–Vis absorption spectra of the copper complex $[\mathbf{Cu(L3)_2}]$ with and without CT-DNA in Tris buffer solution

Table 5 Interactions of the complexes with CT-DNA from UV–Vis spectroscopy

Complex	λ_{max}/nm		Δλ/nm	H%	K_b/M^{-1}
	Free	Bound			
$[\mathbf{Cu(L1)_2}]$	434.0	433.5	0.5	7.5	6.2×10^4
$[\mathbf{Cu(L2)_2}]$	438.0	437.4	0.6	4.5	5.4×10^4
$[\mathbf{Cu(L3)_2}]$	440.0	437.5	1.8	10.5	7.2×10^4
$[\mathbf{Cu(L4)_2}]$	439.0	437.5	1.5	8.0	6.4×10^4

H% = Hyperchromism; Δλ = Bathochromic shift

CT-DNA, the UV–Vis absorption spectra of all four complexes showed increase in absorbance, together with a bathochromic shift (~0.5 nm) with hyperchromism with respect to the control (0 µl DNA). The changes in absorbance values with increasing amounts of CT-DNA were used to evaluate the intrinsic binding constant K_b (Table 5).

It is evident from Table 5 that all four complexes bind to DNA with high affinities such that the estimated binding constants are in the range $5.4 - 7.2 \times 10^4$ M^{-1}. The K_b values of these complexes are comparable with the reported values for redox active Cu(II) pyridine-based tetrazolo[1,5-a]pyrimidine complexes [22]. The intrinsic binding constant for *cis*-platin, which shows a hyperchromic shift in the presence of CT-DNA, is reported as 3.20 10^4 M^{-1} [23].

The interaction of the present complexes with DNA is most likely via π-stacking interactions of the planar pyridyl tetrazole rings. Binding of these complexes to CT-DNA by external contact (electrostatic or groove binding) brought about a bathochromic shift with hyperchromism [24].

Antioxidant activity

The in vitro antioxidant activities of the pyridine tetrazole derivatives and their complexes were evaluated using a reported p-NDA radical scavenging method [25]. The free radical scavenging activities of the compounds were evaluated through their ability to bleach *p*-NDA using ascorbic acid as a reference standard. Potencies for the antioxidant activities of the test compounds compared to ascorbic acid as a reference are given in Table 6. In general, all the present compounds were moderately more potent than the reference. The complex $[\mathbf{Cu(L4)_2}]$ showed highest antioxidant activity.

Conclusions

Pyridyl–tetrazole ligands with acetoamide and acetohydrazide pendant arms and their copper complexes were synthesized and characterized. Physicochemical and spectral studies suggest square planar copper(II) geometries. All four complexes are avid binders of CT-DNA and also have antioxidant properties. These ligands provide a useful

Table 6 *p*-NDA radical scavenging activities of pyridine tetrazole ligands and their complexes

Compound	% radical scavenging method concentrations mg/ml					
	0.5 mg/ml	1 mg/ml	1.5 mg/ml	2 mg/ml	2.5 mg/ml	IC-50 mg/ml
L1	28.47	32.43	39.28	39.84	40.72	3.7
L2	25.36	30.45	32.67	33.87	35.91	5.24
L3	23.8	37.38	37.84	40.04	40.66	3.43
L4	40	40.49	40.34	44.73	42.91	5.76
$[\mathbf{Cu(L1)_2}]$	39.6	40.06	44.16	44.23	44.24	4.3
$[\mathbf{Cu(L2)_2}]$	37.8	38.7	39.26	42.13	45.29	4.04
$[\mathbf{Cu(L3)_2}]$	36.26	36.04	36.35	39.05	39.31	8.38
$[\mathbf{Cu(L4)_2}]$	59.54	54.64	10.16	3.3	42.29	2.815
Ascorbic acid	32.3	56.78	80.45	82.34	85.46	0.64

template for further derivatization with a view to the development of more potent and selective antioxidants and DNA-binding agents.

Acknowledgments SM, MSB and KSR are thankful to the financial assistances from DST with project No.SB/FT/CS-034/2012 (SERB, New Delhi, India) and UGC with project F.No. 42-306/2013 (SR) (New Delhi, India).

References

1. Bhat MR, Jeddi NM, Patil MWA (2011) Asian J Biomed Pharm Sci 1:13
2. Sheridan U, Gallagher JF, Bjerrum MJ, Fleming A, Kelleher F, McGinley J (2014) J Inorg Chim Acta 421:200
3. Popova EA, Trifonov RE, Ostrovskii VA (2012) ARKIVO 1:45
4. Reddy M, Gowd MB, Pasha MA (2011) J Chem Sci 123:75
5. George S, Varma PS, Suresh I, Shanmugapandiyan P (2012) Asian J Pharm Clin Res 5:81
6. Mautner FA, Gspan C, Gatterer K, Goher MAS, Abu-Youssef MAM, Bucher E, Sitte W (2004) Polyhedron 23:1217
7. George S, Shanmugapandiyan P (2012) Int J Pharm Sci 4:104
8. Akhlaghinia B, Rezazadeh S (2012) J Braz Chem Soc 23:2197
9. George S, Shanmugapandiyan P (2013) Int J Chem Tech Res 5:2603
10. Mustafa S, Rao BU, Surendrababu MS, Raju KK, Rao GN (2015) Chem Biodivers 12:1516
11. Reichmann ME, Rice SA, Thomas CA, Doty P (1954) J Am Chem Soc 76:3047
12. Wolfe A, Shimer GH, Meehan T (1987) Biochemistry 26:6392
13. Bond AD, Fleming A, Gaire J, Kelleher F, McGinley J, McKee V, Sheridan U (2012) Polyhedron 33:289
14. Fleming A, Kelleher F, Mahon MF, McGinley J, Prajapati V (2005) Tetrahedron 61:7002
15. Geary WJ (1971) Coord Chem Rev 7:81
16. Butler RN, Fleming AFM (1997) J Heterocycl Chem 34:691
17. Hathaway BJ (1987) In: Wilkinson G, Gillard RD, Mecleverty JA (eds) Comprehensive coordination chemistry, vol 5. Pergamon press, Oxford, p 583
18. Gaponik PN, Voitekhovich SV, Lyakhov AS (2000) Chem Heterocycl Comp 36:326
19. Hughes MN, McWhimmie WR (1966) J Inorg Nucl Chem 28:1659
20. Hathaway BJ, Tomlinson AAG (1970) Coord Chem Rev 5:1
21. Nagaj J, Kamila S-S, Ewa K, Tomasz F, Małgorzata J-B, Wojciech B (2013) Inorg Chem 52:13927
22. Haleel A, Arthi P, Reddy ND, Veena V, Sakthivel N, Arun Y, Perumal PT, Rahiman AK (2014) RSC Adv 4:60816
23. Arjmand F, Sayeed F, Muddassir M (2011) J Photochem Photobiol B Biol 103:166
24. Skyrianou KC, Perdih F, Turel I, Kessissoglou DP, Psomas G (2010) J Inorg Biochem 104:161
25. Barry H, John MCG, Okeizie IA (1987) Anal Biol Chem 165:215